1 Patient Study

1.1 Introduction

As described in section **REF** stereotactic body-radiation therapy with photons (SBRT) showed very promising results for treating non-small cell lung cancer (NSCLC) [Baumann et al., 2009, Fakiris et al., 2009, Grutters et al., 2010, Ricardi et al., 2010, Timmerman et al., 2010, Greco et al., 201
In chapter **REF** was showed that particle therapy (PT) can produce sharp dose gradients with a finite range of the beam and can thus provide higher healthy tissue sparing. This reduces both side effects as well as the risk of secondary cancer [Newhauser and Durante, 2011]. Treatment of lung tumors with PT is still challenging due to interplay and radiological path length changes (see section **REF**. Nevertheless, in recent years there have been several clinical studies using PT on lung tumors with promising results [Tsujii and Kamada, 2012]. It is important to note that all of these studies used passive beam scattering avoiding the problem of interplay between organ motion and scanning beam motion. However, the active beam scanning can provide even better dose shaping which becomes even more important in high dose single fractionation regimes. Therefore an in silico comparison between photon and active scanning ion carbon therapy (CiT) for NSCLC was conducted and will be presented in this chapter.
We hypothesize that (a) CiT could provide better healthy tissue sparing than photons in treating lung tumors or metastases due to its favorable dose profile. (b) Patient characteristics can be identified that allow the selection of patients especially suited for CiT. To evaluate our hypothesis, an in silico comparison of simulated CiT plans to single dose SBRT (SDRT) plans actually delivered was performed. Target coverage and a wide range of OAR doses were assessed both with and without simulated motion on 4DCTs.

1.2 Materials and methods

In this section input data will be presented as well as treatment planning parameters and procedures for SDRT and CiT. Finally, analysis method will be described.

1.2.1 Patient data

Study included 19 patients with in total 26 lesions that were actually treated with SDRT at the Fundaçao Champalimaud. The lesion size was 2.9 cm^3 (median, 25-75% 1.4 - 9.7) and

peak-to-peak motion was 3.1 mm (1.6 - 5.6). Three patients had two targets, one had five and the rest one. 13 lesions were right-sided and 12 were left-sided and one was located in right cardiophrenic space. An overview of tumor characteristics can be found in Table **??**. Two computed tomographies (CT) were available for all patients. A planning CT was used for OAR delineation and SDRT planning. Target motion was estimated on a second, time-resolved CT (4D-CT), consisting of 10 motion phases. Clinical target volumes (CTV) were delineated using a registered positron emission tomography (PET) scan. The planning objectives were that 99 % of planning target volume (PTV) must receive at least 24 Gy (V99% $\geq$ 24 Gy) in a single fraction, while all OAR constraints as defined in the AAPM task group 101 report on stereotactic radiotherapy had to be respected [Benedict et al., 2010]. Different PTV definitions were used in SDRT and CiT, due to CiT sensitivity to range changes. The definitions are described in next section.

Table 1.1: Lesion characteristics, with lesion locations, stages, peak-to-peak motions and volumes of corresponding CTV, SPTV and FTV. Abberevations for lesion location are: RSL, right superior lung; IRL, inferior right lung; LSL, left superior lung; ILL, inferior left lung; RCS, right cardiophrenic space.

Number	Location	Stage	Peak-to-peak motion [mm]	Volume (cm^3)		
				CTV	SPTV	FTV
1	LSL	IIa	4.8	35.9	100	179
2	LSL	Ia	3.1	1.6	7.7	40.6
3	IRL	IV	12	2.3	11.6	32
4	RSL	Ia	0.5	6.9	25.2	38
5	ILL	IV	4.4	2.5	15	20.5
6	ILL	IV	7.5	1.4	7.7	26.5
7	RSL	IV	3.9	16	40	72.5
8	ILL	IV	0.6	139	261	255
9	LSL	IV	2	9.2	35	46.5
10	IRL	IV	3.4	10.2	38	45.5
11	ILL	IV	2.8	14.4	46.4	57.2
12	ILL	IV	5.8	3.8	17.4	23.4
13	RSL	IV	0.8	4.3	17.7	26.3
14	LSL	IV	3.4	2.7	14.5	23.1
15	RSL	IV	2.1	3.1	15.4	33.5
16	LSL	IV	0.5	0.5	5.4	6.7
17	ILL	IV	7.8	0.8	6.1	23.5
18	LSL	IV	0.1	1.7	15	23.5
19	IRL	IIIb	11.4	27	137	118.5
20	RSL	Ia	2.2	1.7	10	23.4
21	RSL	IV	0.2	0.9	3.2	14.9
22	RSL	IV	2.2	3.9	22.1	27.5
23	LSL	IV	3.1	9.8	28	51
24	RSL	IV	8.1	0.6	3.3	4.1
25	LSL	IV	1.4	0.8	5.9	10
26	RCS	IV	11.8	0.4	6.6	8.6

1.2.2 Planning target volume definition

To account for range changes relevant for particles only, different PTV definitions were used for SDRT and CiT, as shown in Figure **MISSING**. Within this thesis they will be named SPTV and FTV (field-specific target volume) for SDRT and CiT, respectively. In SDRT, the responsible clinician determined the maximum breathing motion of the CTV from the 4DCT, hence creating an ITV. This ITV plus an additional 3 mm for setup uncertainty yielded the SPTV.

FTV was constructed following principles from Graeff et al [Graeff et al., 2012]. Each beam has a unique FTV. For setup uncertainty margins of 3 mm laterally and 1 mm in beam's eyes

view (BEV) were used on the CTV. Afterwards a water-equivalent path length ITV (WEPL-ITV) was build, using transformation maps from the B-Spline deformable registration of the 4DCT data [Shackleford et al., 2010]. Additional 2 mm + 2 % proximal and distal margins were added in BEV to account for uncertainty from Hounsfield units to water equivalent path length conversion.

If the target overlapped with an OAR (e.g. small airways) then OAR plus a margin of 2-5 mm was subtracted from SPTV or FTV, to satisfy OAR constraints.

1.2.3 SDRT treatment planning

The clinical plans were calculated with the Eclipse v10 planning system (Varian Medical Systems, Palo Alto, Ca, USA) using the AAA algorithm. All plans delivered 24 Gy, generally using 4 VMAT partial arcs. For tumor sizes > 2.5 cm a calculation grid of 2.5 mm was used, otherwise it was 1 mm. During optimization, a first iteration included the SPTV only, after which the OARs were added. In order to lower OAR dose and improve the SPTV homogeneity,an artificial shell of 2 cm around the SPTV was created and the dose was minimized there as well. Finally, an intermediate dose calculation with AAA was mandatory to get an adequate SPTV coverage after optimization.

1.2.4 CiT treatment planning

For CiT, state of the art 4D treatment planning software TRiP4D was used (see section **REF**). A single field uniform dose plan (SFUD) was optimized on the FTV in the end-inhale reference phase of the 4D-CT. Dose was then calculated on end-inhale (3D-0%) and end-exhale (3D-50%) phases. 4D dose delivery was simulated over the whole breathing cycle with two different breathing periods (3.6 and 5 s) and two different starting phases (0° and 90°). Simulations without motion compensation (4D-interplay) and with slice-by-slice rescanning were performed (4D-rescans). Five rescans were used for the majority of targets (n=24), whereas 20 rescans were used for targets (n=2) where the interplay effects were too big to achieve a satisfactory target coverage.

Dose was computed considering the relative biological effectiveness (RBE) following the local effect model (LEM) IV [Elsaesser et al., 2010]. The Alpha beta ratio was chosen conservatively, withion a ratio of 10 Gy and 2 Gy for target and OARs, respectively. This led to RBE of approximately 1.1 in target tissue and approximately 1.1 to 3 in OARs. An example RBE distribution is shown in Fig. 1.1

Most targets (n=20) were planned with two fields. For remaining targets, one (n=1), three (n=3) or four (n=2) fields were used due to proximity of OARs. A beam spot spacing of 2 mm,

a focal size of approximately 6 mm (FWHM), a 3 mm ripple filter and in most cases a bolus of a 80 mm width were used.

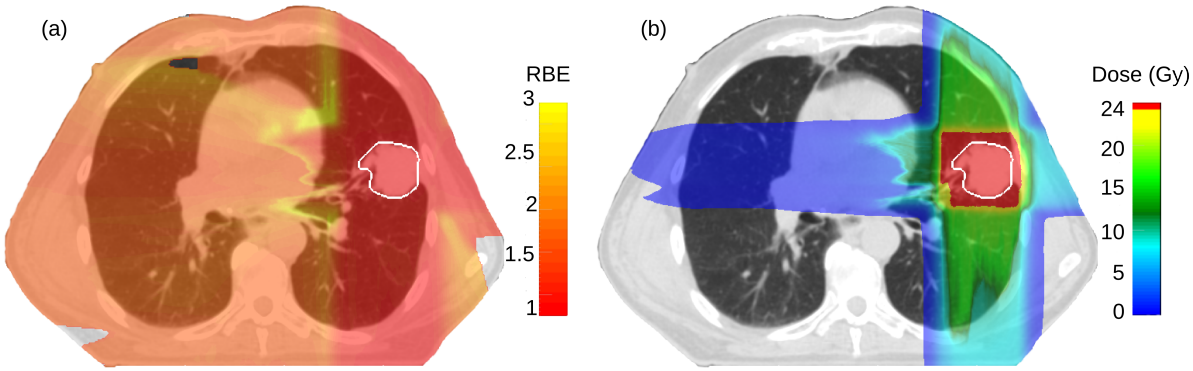

Figure 1.1: RBE distribution in a patient (a) depends on a actual dose profile (b).

1.2.5 Dose metrics and analysis

For comparison between SDRT and CiT the following dose metrics were used - relative volume of the CTV receiving 100 % of prescribed dose (V_{100}%), the minimum dose in 95% of the volume ($D_{95\%}$), the maximum point dose (D_{Max}), and the mean dose (D_{Mean}). The first two metrics, V_{100}% and $D_{95\%}$ were used to compare target coverage, whereas OAR dose was compared with DMax and DMean.

For 4D CiT dose calculations, mean and standard deviation were calculated for different breathing periods and starting phases.

Paired t-tests were performed to compare the dose metrics and for post-hoc exploratory analysis between groups a two-sided t-test with Welch correction for different variances as carried out. A p-value < 0.05 was considered significant. Dose differences are always reported such that higher dose levels for SDRT result in positive values.

1.3 Results

Examples of two SDRT and 4D-rescan CiT treatment plans are shown in Figure **REF**. Patient A has two lesions in close proximity to the spinal cord. Patient B has a small lesion (0.87 cc) in the superior position of the left lung wing. V_{100}% is 100% for SDRT and CiT in all CTVs for Patient A and B; average OAR difference between SDRT and CiT in D_{Max} is 5.3 Gy and 1.5 Gy and in D_{Mean} 1.2 Gy and 0.6 Gy, respectively for patient A and B.

1.3.1 Target Coverage

Difference in PTV definition resulted in 1.5 (1.3 - 2.1) times bigger FTV than SPTV. There was no significant difference in CTV $D_{95\%}$ between SBRT and any CiT calculation. For CTV V_{100}% there was a significant difference between SDRT and 4D-interplay, 3.8 (0 - 6.1)% and no significant difference between SDRT and 3D-0%, 3D-50% or 4D-rescan. Difference in V100% between 4D-rescan and 4D-interplay with respect to CTV peak-to-peak motion and average CTV range change in water is plotted in Figure 3. Range change was a better predictor of the V_{100}% difference than geometric motion (r=0.75 vs. r=0.48). There was a significant difference in V_{100}% standard deviation between 4D-interplay and 4D-rescans, 1.8 (0 - 2.9)%, i.e. interplay simulation showed a larger variability in dose coverage in addition to the difference in averages.

1.3.2 Dose in OARs

There was no significant difference in dose to OAR between the different CiT dose calculations. The dose metrics for SDRT and 4D-rescan CiT for OARs heart, spinal cord, smaller airway esophagus, trachea, aorta, ipsi- and contralateral lung are presented in Table 2. In almost all patients CiT deposited less dose in all OARs, except ipsilateral lung, where there was no statistical significant difference between SDRT and CiT. The average OAR difference between SDRT and CiT was significant, 2.5 (0.3- 4.8) Gy for D_{Max} and 0.6 (0.2- 1.7) Gy for D_{Mean}. The contralateral lung did not receive any dose in 12 (71%) patients with CiT.

Table 1.2: Dose metrics for OARs. First value at each organ is from SDRT and the second from 4D-rescan. All values are shown as median and 25-75% in brackets.

	D_{Max} (Gy)		D_{Mean} (Gy)	
OAR	Photon	Carbon	Photon	Carbon
Heart	15.0 (11.9 - 21.8)	10.8 (3.3 - 13.2)	1.3 (0.1 - 2.2)	0 (0 - 0.2)
Spinal Cord	9.3 (8.7 - 10.4)	0 (0 - 5.9)	0 (0 - 0.3)	0 (0 - 0)
Smaller Airways	15.0 (13.4 - 20.2)	10.9 (1.9 - 13.5)	2.8 (1.5 - 5.8)	0.7 (0 - 1.9)
Esophagus	11.0 (9.0 - 12.6)	0 (0 - 0.7)	1.1 (0.6 - 1.5)	0 (0 - 0)
Aorta	19.3 (10.1 - 25.5)	7.5 (2.0 - 14.3)	1.4 (0.7 - 1.6)	0 (0 - 0.1)
Ipsilateral Lung	26.3 (26.0 - 26.5)	26.3 (25.8 - 26.8)	2.3 (1.5 - 3.1)	2.5 (1.6 - 3.4)
Contralateral Lung	4.8 (3.5 - 6.8)	0 (0 - 0.3)	0.4 (0.2 - 0.6)	0 (0 - 0)

	D_{Max} (Gy)		D_{Mean} (Gy)	
OAR	Photon	Carbon	Photon	Carbon
Heart	15 (11.9 - 21.9)	10.9 (3.3 - 13.2)	4.7 (3.7 - 6.3)	0.1 (0.1 - 0.9)
Spinal Cord	9.3 (8.7 - 10.4)	0 (0 - 5.9)	2.0 (1.4 - 2.3)	0 (0 - 0)
Smaller Airways	15.0 (13.4 - 20.2)	10.8 (1.9 - 13.5)	2.8 (2.6 - 5.9)	0.9 (0.3 - 1.7)
Esophagus	11.0 (9.0 - 12.7)	0 (0 - 0.7)	3.8 (2.4 - 4.4)	0 (0 - 0)
Aorta	19.3 (10.1 - 25.5)	7.5 (2.0 - 14.3)	3.5 (2.1 - 4.9)	0.1 (0 - 0.7)

Bibliography

[Baumann et al., 2009] Baumann, P., Nyman, J., Hoyer, M., Wennberg, B., Gagliardi, G., Lax, I., Drugge, N., Ekberg, L., Friesland, S., Johansson, K. A., Lund, J. A., Morhed, E., Nilsson, K., Levin, N., Paludan, M., Sederholm, C., Traberg, A., Wittgren, L., and Lewensohn, R. (2009). Outcome in a prospective phase ii trial of medically inoperable stage i non-small-cell lung cancer patients treated with stereotactic body radiotherapy. *Journal of Clinical Oncology*, 27(20):3290–3296.

[Benedict et al., 2010] Benedict, S. H., Yenice, K. M., Followill, D., Galvin, J. M., Hinson, W., Kavanagh, B., Keall, P., Lovelock, M., Meeks, S., Papiez, L., Purdie, T., Sadagopan, R., Schell, M. C., Salter, B., Schlesinger, D. J., Shiu, A. S., Solberg, T., Song, D. Y., Stieber, V., Timmerman, R., Tome, W. A., Verellen, D., Wang, L., and Yin, F. F. (2010). Stereotactic body radiation therapy: the report of aapm task group 101. *Medical Physics*, 37(8):4078–4101.

[Elsaesser et al., 2010] Elsaesser, T., Weyrather, W. K., Friedrich, T., Durante, M., Iancu, G., Krämer, M., Kragl, G., Brons, S., Winter, M., Weber, K. J., and Scholz, M. (2010). Quantification of the relative biological effectiveness for ion beam radiotherapy: direct experimental comparison of proton and carbon ion beams and a novel approach for treatment planning. *Int. J. Radiat. Oncol. Biol. Phys.*, 78(4):1177–1183.

[Fakiris et al., 2009] Fakiris, A. J., McGarry, R. C., Yiannoutsos, C. T., Papiez, L., Willams, M., Henderson, M. A., and Timmerman, R. (2009). Stereotactic body radiation therapy for early-stage non-small-cell lung carcinoma: four-year results of a prospective phase ii study. *International Journal of Radiation Oncology*, 75(3):677–682.

[Graeff et al., 2012] Graeff, C., Durante, M., and Bert, C. (2012). Motion mitigation in intensity modulated particle therapy by internal target volumes covering range changes. *Medical Physics*, 39(10):6004–6013.

[Greco et al., 2011] Greco, C., Zelefsky, M. J., Lovelock, M., Fuks, Z., Hunt, M., Rosenzweig, K., Zatcky, J., Kim, B., and Yamada, Y. (2011). Predictors of local control after single-dose stereotactic image-guided intensity-modulated radiotherapy for extracranial metastases. *Int.J.Radiat.Oncol.Biol.Phys.*, 79(4):1151–1157.

[Grutters et al., 2010] Grutters, J. P. C., Kessels, A. G. H., Pijls-Johannesma, M., Ruysscher, D., oore, M. A. ., and Lambin, P. (2010). Comparison of the effectiveness of radiotherapy with

photons, protons and carbon-ions for non-small cell lung cancer: A meta-analysis. *Radiotherapy and Oncology*, 95(1):32–40.

[Newhauser and Durante, 2011] Newhauser, W. D. and Durante, M. (2011). Assessing the risk of second malignancies after modern radiotherapy. *Nat.Rev.Cancer*, 11:434–448.

[Ricardi et al., 2010] Ricardi, U., Filippi, A. R., Guarneri, A., Giglioli, F. R., Ciammella, P., Franco, P., Mantovani, C., Borasio, P., Scagliotti, G. V., and Ragona, R. (2010). Stereotactic body radiation therapy for early stage non-small cell lung cancer: Results of a prospective trial. *Lung Cancer*, 68(1):72–77.

[Shackleford et al., 2010] Shackleford, J. A., Kandasamy, N., and Sharp, G. C. (2010). On developing b-spline registration algorithms for multi-core processors. *Physics in Medicine and Biology*, 55(21):6329–6351.

[Timmerman et al., 2010] Timmerman, R., Paulus, R., Galvin, J., Michalski, J., Straube, W., Bradley, J., Fakiris, A., Videtic, G., Johnstone, D., Fowler, J., Gore, E., and Choy, H. (2010). Stereotactic body radiation therapy for inoperable early stage lung cancer. *JAMA*, 303(11):1070–1076.

[Tsujii and Kamada, 2012] Tsujii, H. and Kamada, T. (2012). A review of update clinical results of carbon ion radiotherapy. *Jpn.J.Clin.Oncol.*, 42(8):670–685.